REDISTRIBUTION OF CARBON IN STEELS DURING LONG-TERM OPERATION OF EQUIPMENT IN HYDROGEN-CONTAINING ENVIRONMENTS

A. V. Nechaeva[1, a, *], L. G. Vagina[2, b], A. M. Polyansky[3, c], V. A. Polyansky[4, d],
V. V. Shalagaev[1, 4, e], and Yu. A. Yakovlev[4, f]

[1]Russian Laboratory Ltd, 9/A, 3-N, 1 Pushkarskiy Lane, Saint Petersburg, 197101, Russia
[2]Gazprom neftekhim Salavat LLC,
30 Molodogvardeitsev St., Salavat, Rep. of Bashkortostan, 453256, Russia
[3]Electronic and Beam Technologies LLC,
29 Politekhnicheskaya St., Saint Petersburg, 194021, Russia
[4]Institute of Problems in Mechanical Engineering of the Russian Academy of Sciences,
61 Bolshoy Ave., Vasilievskiy Island, Saint Petersburg, 199178, Russia

[a] https://orcid.org/0009-0005-2617-9736 ✉ pomazova@yandex.ru;
[b] https://orcid.org/0009-0001-8470-1191 ✉ chayka29@gmail.com;
[c] https://orcid.org/0000-0002-6470-9583 ✉ ampol@electronbeamtech.com;
[d] https://orcid.org/0000-0002-1199-1028 ✉ vapol@mail.ru;
[e] https://orcid.org/0009-0004-9558-9539 ✉ Vladimir.Shalagaev@ruslab.org;
[d] https://orcid.org/0000-0002-5041-0441 ✉ yura.yakovlev@gmail.com

*Corresponding author. Email: pomazova@yandex.ru
Address for correspondence: Pushkarskiy per., 9/A, 3-N, 1, Saint Petersburg, 197101, Russia
Tel.: +7 (913) 619-5203

The effect of carbon redistribution during long-term operation of equipment operating in different hydrogenating environments and at different operating pressures is described. It was revealed that microstructural decarburization in damaged equipment was caused by carbon diffusion from the pearlite grain body and its accumulation along the grain boundaries. In this case, the average concentration of carbon did not change. This effect was confirmed by a complex of tests: optical emission analysis, optical and electron microscopy, energy-dispersive analysis of the structural components on polished metallographic sections, elemental mapping of surfaces obtained as a result of impact tests of the analyzed samples. It is shown that the pattern of the diffusive redistribution of carbon did not depend on the composition of the working medium (organic and inorganic substances and their mixtures), but resulted from industrial equipment operation time under external load.

Keywords: hydrogen embrittlement, microstructure decarburization, equipment damage

1. Introduction

Decarburization of steels is considered to be one of the main symptoms of irreversible hydrogen brittleness [1–4]. This effect was described for the first time in 1941 [4] as a result of high-temperature hydrogen attack on steel, which took place at high temperatures and pressures of a hydrogen-containing environment. Extensive studies of the effect of high-temperature hydrogen attack on steels conducted over the past 80 years have shown that hydrogen-induced decarburization is a part of the phenomenon of high-temperature hydrogen attack [2]. It was found that, at high temperatures and pressures of hydrogen in the environment, the decarburization of steels occurs very quickly. The safe maximum operating temperature curves versus hydrogen pressure in the environment (Nelson diagrams) were plotted and standardized (API 941 2016) for steel structures.

According to modern research, removal of carbon from steels or significant decrease in its concentration is one of the results of almost any saturation of steels with hydrogen [5–13]. This occurs both at high [9, 11–13] and low [5, 6] temperatures and pressures of a hydrogen-containing medium. Dissolved hydrogen accumulated by steel is considered as the main carbon absorber [1, 2, 4–15]. The main chemical reactions of decarburization are written as follows:

$$4H^+ + Fe_3C \rightarrow CH_4 + 3Fe \tag{1}$$

$$4H^+ + C \rightarrow CH_4. \tag{2}$$

Hydrogen accumulation inside the steel leads to the decomposition of pearlite, resulting in the formation of voids that are filled with methane formed by the reactions of dissolved hydrogen with iron carbide and carbon (1)–(2). Accumulation of methane in the voids leads to methane disease of steel [1, 16, 17].

In the works of E. Lunarska [14] it is indicated that voids are filled not with pure methane, but with a mixture of methane with water and molecular hydrogen. An independent study of the composition of gas released from cast iron, zinc, and iron samples after their saturation with hydrogen by cathodic polarization, described in [15], showed that, when hydrogen interacts with steel, not only methane is formed, but also a significant amount of other hydrocarbons (from ethane to hexane). Methane and other gaseous substances formed during hydrogen decarburization inside steel lead to carbon removal from the internal microstructure (decomposition of microstructural elements) and a significant decrease in the average carbon concentration in a metal [1, 14, 15].

It is known that decarburization also occurs during heating, tempering, and annealing of steels in air [18–22] due to structural transformations of martensite, decomposition of carbides and ferrites, diffusion of carbon to grain boundaries and its oxidation. It is known that breakdown of pearlites and decomposition of iron carbides, in their turn, increase the susceptibility of steels to dissolved hydrogen, too [18, 23–26]. Thus, the hydrogen decarburization process contains an additional feedback, which increases its destructive effect.

The main contradiction of the generally recognized mechanism of hydrogen decarburization is the discrepancy between the values of initial carbon concentrations and the accumulated hydrogen concentration in steels. For methane formation, it is necessary that there be four times as many hydrogen atoms as carbon atoms. However, it was found experimentally and reliably that the maximum concentration of dissolved hydrogen in steels is hundreds of times less than the usual concentration of carbon [5–10]. That is, the probability of chemical reactions (1)–(2) is low. Consequently, the loss of carbon and iron carbides due to the formation of methane will occur very slowly.

All the effects associated with the loss and transformation of carbon in steels are of great practical importance since carbon is an element which determines the hardness, strength, creep, and ductility of carbon steels, and it is most often used in power and chemical equipment.

When we investigated real cases of hydrogen-induced damage that occurred during operation of the equipment, the average carbon concentration did not change at all and corresponded to the steel grade composition [27].

To determine the causes of destruction and to clarify its mechanisms, we studied samples cut out from the walls of equipment destroyed during long-term operation in a hydrogen-containing environment.

2. Materials, equipment, and research methods

Steel samples cut out from the walls of equipment damaged during operation in various hydrogen-containing media, the composition and parameters (temperature, pressure) of which are indicated in Table 1, were used as test objects. The analysis of the fractures showed that the damage to the equipment occurred by the mechanism of hydrogen embrittlement. Data on damaged equipment are shown in Table 1. At the same time, samples made of new metal of the same steel grades

were tested. The letters "D" and "N" were added to the marking of damaged and new samples, respectively. The samples were made meeting the requirements imposed to the equipment components during their manufacture.

Table 1

The analyzed samples

Sample number	Sample No 1D	Sample No 2D	Sample No 3D
Medium	Mixture Isobutylene + water	Stable gas condensate	Steam–water mixture
Steel grade	09G2S	10G2S1	Steel 20
Working medium parameters	$T = 344$ °C, $P = 0.05$ MPa	$T = 40$ °C, $P = 0.6$ MPa	$T = 403$ °C, $P = 15.7$ MPa
Operating time, thousand hours	85	595	171

The chemical analysis of the samples was performed by the method for quantitative elemental composition according to GOST R 54153-2010. A Foundry-Master Smart optical emission analyzer was used.

Metallographic analysis was carried out on plates cut out from the walls of the equipment specially made with the help of the LaboTom-3 cutting machine and the LaboPol-2 grinding and polishing machine (Struers A/S). The presence of recirculation, spray cooling and the multi-stage system of polished specimen preparation allows one to avoid overheating, heat generation, and changes in the structure of a sample during cutting and grinding. The cut-out plates were subjected to cold pouring in epoxy resin, which prevents wrong geometry of edges in the process of grinding and ensures the necessary orientation of the samples. A 4% alcohol solution of HNO_3 was used to identify the structural components of the samples. A metallographic analyzer of fragments of the microstructure of solids, including an inverted Olympus GX53 microscope with SIAMS Photolab software, was used for the morphological analysis of the structural components of steel and the assessment of surface quality. The metallographic analysis examined the plates cut out in such a way that the entire wall thickness was analyzed.

Electron microscopic images of the metal were obtained in secondary electrons on a JEOL JCM-5700 device equipped with a JED-2300 energy dispersion analyzer. The images were also obtained by means of a Tescan Vega 3 LMN scanning electron microscope having an X-ray energy dispersion analysis system with a nitrogen-free X-act ADD detector, secondary electrons obtained using an ET-type detector (YAG crystal). Elemental mapping of the surface was carried out on the halves of impact test samples after impact bending according to GOST 9454-78. An IO-5003-0.3-11 impact pendulum-type testing machine was used.

The mass fraction of hydrogen in the samples was determined in accordance with GOST 17745-90 by vacuum heating using an AV-1 mass spectrometric hydrogen analyzer at two extraction temperatures of 530 °C and 800 °C.

3. The results of experimental studies and discussion

The hydrogen concentration in the metal was measured by the vacuum heating method. Samples for determining the hydrogen concentration were cut out at a distance of □100 mm from the edges of damage (fractures). Hydrogen concentration was measured also in new samples made of the metal in the state of delivery. The measurement results are shown in Table 2. The symbol ΣQ indicates the average (of two parallel measurements) total hydrogen content released at two extraction temperatures. The results obtained confirm that hydrogen accumulation in the metal of the damaged samples occurred during operation. The hydrogen concentration increased by factors of 3.1, 6.7, and 6.5 in samples No 1D, 2D, and 3D, respectively.

Table 2

Nechaeva A. V., Vagina L. G., Polyansky A. M., Polyansky V. Shalagaev A., V. V., and Yakovlev Yu. A. Redistribution of carbon in steels during long-term operation of equipment in hydrogen-containing environments // Diagnostics, Resource and Mechanics of materials and structures. – 2025. – Iss. 1. – P. 011–022. – DOI: 10.17804/2410-9908.2025.1.011-022.

The results of determining the mass fraction of hydrogen, wt%

Sample marking	$\sum Q, M^{-1}$
Sample No 1D	0.3435
Sample No 1N	0.1105
Sample No 2D	0.9488
Sample No 2N	0.1425
Sample No 3D	1.3610
Sample No 3N	0.2105

The initial microstructure of the applied steel grades of the studied samples, corresponding to the metal in the state of delivery, is a ferrite-pearlite one [28]. Ferrite is a solid solution of carbon (up to 0.02%) in б-iron (б-ferrite). Pearlite is a conglomerate of alternating lamels of ferrite and cementite. Cementite (iron carbide) is a chemical compound of iron with carbon (Fe_3C), with a maximum carbon concentration of 6.67%.

Metallographic analysis showed that, during operation, decarburization of the internal structure of steel grains with varying degrees of intensity occurred under the influence of hydrogen. In sample No 1D the microstructure of the sample near the site of destruction of the reactor walls consists of almost pure ferrite (Fig. 1 *a*), carbides being disintegrated completely. In samples No 2D (Fig. 1 *b*) and No 3D (Fig. 1 *c*) only partial decarburization of the microstructure occurred. The decay of the carbide component of the steel within the boundaries of the former pearlite grains is clearly visible in these samples.

All the metal underwent the same phase changes during operation. There is no difference between carbon distribution along the edges of the fractures and that at a distance from them. In sample No 1D microcracks and cracking around these cracks are present, at a distance from the damage (□100 mm), cracking along grain boundaries was not detected (Fig. 2 *a*). Cracking was detected at a distance from the damage in samples No 2D (Fig. 2 *b*) and No 3D (Fig. 2 *c*). It is more intensive in sample No 3D.

As is known [1, 14, 15], when steels are saturated with hydrogen, the latter interacts with cementite to form methane gas, and this should lead to the formation of voids along the grain boundaries and the swelling of the metal. In the samples studied by us, metal swelling and the formation of voids along the grain boundaries due to damage accumulation and accumulation of methane were not detected. The width of the intergranular cracks in all the samples after operation was the same (Fig. 2 *b*, *c*).
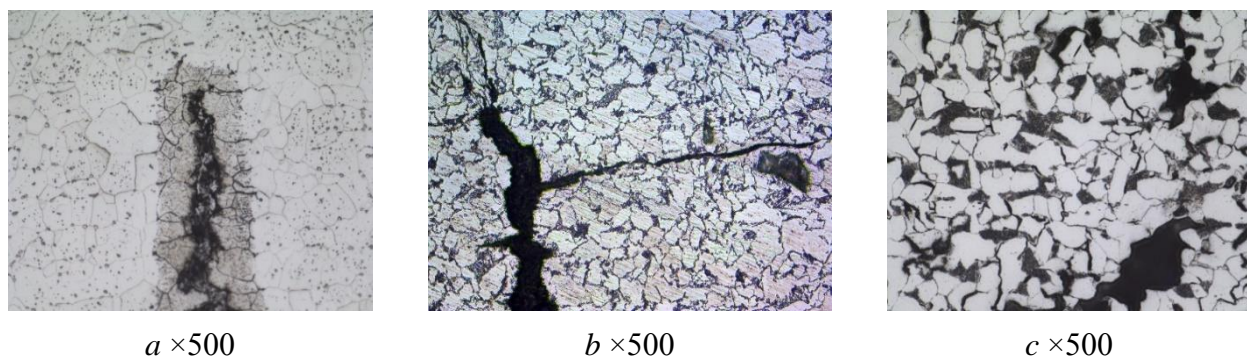

a ×500   b ×500   c ×500

Fig. 1. The microstructures of the samples near the damage: sample No 1D (*a*);
sample No 2D (*b*); sample No 3D (*c*)

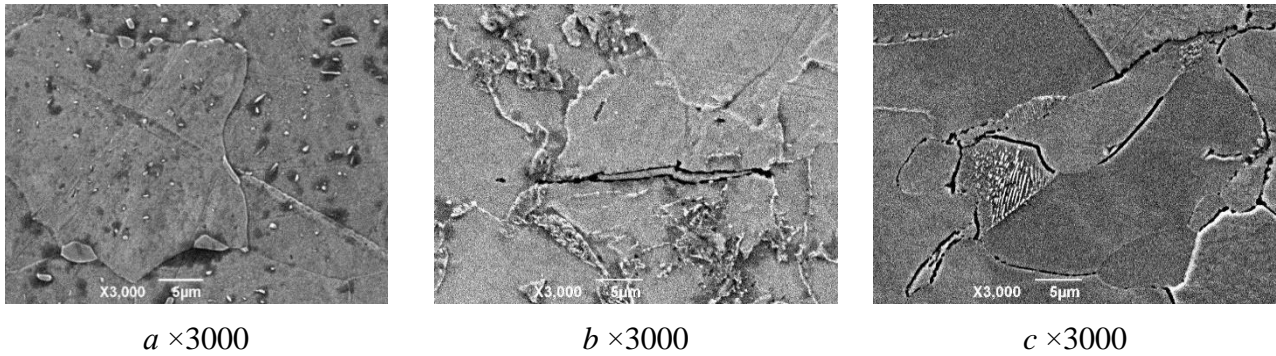*a* ×3000   *b* ×3000   *c* ×3000

Fig. 2. The microstructures of the damaged samples at a distance from the damage: sample
No 1D (*a*); sample No 2D (*b*); sample No 3D (*c*)

The results of optical emission spectral analysis in comparison with the new samples are shown in Table 3. They indicate the absence of decarburization of the metal of the studied samples. This, on the one hand, contradicts the microstructural decarburization observed under a microscope and, on the other hand, explains the absence of symptoms of methane disease. It should be noted that the optical emission analysis inspected the entire wall thickness in every 2 mm. Thus, it was just the average carbon concentration throughout the wall thickness of the equipment that did not differ in the new and operated equipment, and it was at the upper permissible level for the studied steel grades (Table 1). There were no changes in the concentration of the other elements either.

Table 3

Mass fraction of the chemical elements, %

Sample number	C	Mn	Si	Cr	Ni	S	Cu	P	V
Sample No 1D	0.110± 0.016	1.41± 0.06	0.64± 0.05	0.081± 0.011	0.031± 0.008	0.0053± 0.0024	0.016± 0.005	0.014± 0.003	0.0080± 0.0024
Sample No 1N	0.112± 0.016	1.42± 0.06	0.64± 0.05	0.080± 0.011	0.029± 0.008	0.0052± 0.0024	0.016± 0.005	0.015± 0.003	0.0080± 0.0024
Norms for steel 09G2S as per GOST 19281-2014	≤0.12	1.3–1.7	0.50–0.80	≤0.30	≤0.30	≤0.035	≤0.30	≤0.030	≤0.12
Sample No 2D	0.122± 0.016	1.47± 0.06	1.07± 0.08	0.117± 0.016	0.082± 0.012	0.0048± 0.0012	0.128± 0.020	0.024± 0.006	0.0042± 0.0016
Sample No 2N	0.124± 0.016	1.45± 0.06	1.01± 0.08	0.105± 0.016	0.090± 0.012	0.0051± 0.0024	0.115± 0.020	0.032± 0.006	0.0049± 0.0016
Norms for steel 10G2S1 as per GOST 19281-2014	≤0.12	1.30–1.65	0.80–1.1	≤0.30	≤0.30	≤0.035	≤0.30	≤0.030	≤0.12
Sample No 3D	0.232± 0.024	0.445± 0.024	0.26± 0.03	0.028± 0.006	0.008± 0.003	0.0042± 0.0016	0.012± 0.005	0.020± 0.003	–
Sample No 3N	0.222± 0.024	0.435± 0.024	0.28± 0.03	0.031± 0.006	0.007± 0.003	0.0032± 0.0016	0.015± 0.005	0.024± 0.003	–
Norms for steel 20 as per GOST 1050-2013	0.17–0.24	0.35-0.65	0.17–0.37	≤0.25	≤0.30	≤0.035	≤0.30	≤0.030	–

There is a contradiction among the microstructural decarburization that we have discovered, the absence of symptoms of methane disease, and the absence of changes in the average carbon concentration.

Nechaeva A. V., Vagina L. G., Polyansky A. M., Polyansky V. Shalagaev A., V. V., and Yakovlev Yu. A. Redistribution of carbon in steels during long-term operation of equipment in hydrogen-containing environments // Diagnostics, Resource and Mechanics of materials and structures. – 2025. – Iss. 1. – P. 011–022. – DOI: 10.17804/2410-9908.2025.1.011-022.

To clarify this contradiction, an energy dispersive analysis was carried out along the boundaries of the decarburized grains of the samples. To do this, the boundaries between the grains were analyzed, which have a significant difference in thickness. As the published data show, energy dispersive analysis is effective for solving such problems. For example, in [29] this analysis was successfully used to prove the restoration of cementite in the surface layer (up to 10 мм) after dehydrogenization, and in [30] the redistribution of carbides in the 12Cr1MoV steel after long-term high-temperature operation was proved.

The area of energy dispersion analysis (EDS) went beyond the grain boundaries and covered the ferritic grains; therefore, only the lower concentration limit of the carbon content at the grain boundaries was determined. Electron microscopic images indicating the areas of analysis are shown in Fig. 3. The results of the analysis are summarized in Table 4.
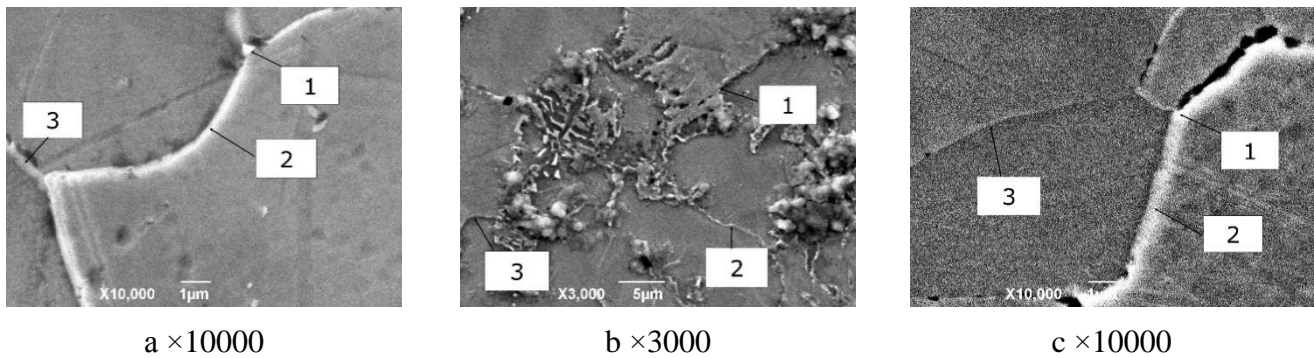

a ×10000   b ×3000   c ×10000

Fig. 3. Electron microscopic images of the metal samples transmitted in secondary electrons, indicating the locations of EDS analysis: sample No 1D (*a*); sample No 2D (*b*); sample No 3D (*c*)

Table 4

Carbon concentration at grain boundaries, %

Sample number	Sample No 1D	Sample No 2D	Sample No 3D
Boundary of three grains (area of analysis No 1)	≥11.5	≥9.0	≥9.9
Thickened boundary of two grains (area of analysis No 2)	≥8.5	≥7.9	≥8.2
Thin grain boundary (area of analysis No 3)	≥4.4	≥4.8	≥1.6

According to the above photos and the data of Table 4, it can be seen that, during operation of the equipment, carbon atoms diffused from pearlite to grain boundaries. The maximum carbon concentration was recorded by us along the boundary of three grains, and it was 11.5, 9.0, and 9.9% for samples Nos 1D, 2D, and 3D, respectively. The concentrations obtained correlate with the microstructural studies, where the degree of grain decarburization was maximal in sample No 1D.

Since carbon could get to the fractures of the walls of the equipment from the working medium, during transportation, etc., in order to confirm the fact of carbon accumulation along the boundaries of the metal grains additionally, elemental mapping was carried out for the fracture surfaces formed after impact tests (according to GOST 9454-78) of the samples cut out from the walls of the equipment. These tests were carried out by us under "clean conditions", which eliminate contamination of the analyzed surface of the samples before, during and after destruction due to impact bending.

The results obtained for the "destroyed" samples were compared with those for the "new" samples.

The elemental mapping of the surfaces was carried out in the center of the fractures in 5 areas. The electron microscopic images of the surfaces of samples No 1D and No 1N are shown in Fig. 4. The values of carbon concentration in the analyzed fields are shown in Table 5. A good convergence in carbon concentration at different control sites within the same sample was obtained. With

the initial equality in the carbon concentration in new and damaged samples No 1, the carbon concentration on the fracture surface in the damaged samples is 2.5 times as high. Similar results were obtained when comparing the results of the analysis of the fractures in damaged and new samples No 2 and No 3, where the carbon concentration along the grain boundaries in the damaged equipment exceeded that in the new samples for certain.

Carbon can diffuse in steels just under the influence of mechanical loads. In [31] the redistribution of carbon atoms during deformation of steel 20 under load was demonstrated. Deformation leads to the destruction of cementite particles located at the boundaries of dislocation fragments and to the formation of carbides inside the fragments. Carbon from the destroyed cementite particles at the boundaries of the fragments finds its place in the formation of cementite particles inside the fragments, in defects of the crystal lattice, and in formation of carbides in new morphological structures. Similar results were obtained in [32], where the processes of redistribution of carbon atoms in the solid solution, cementite particles, and elements of defective substructure occurred under the influence of surface load.

Carbon diffuses from the grain body and accumulates along the grain boundaries. Based on the close values of carbon concentration in the new and damaged samples, average throughout the entire wall section, the data obtained suggest that the redistribution of carbon under load during operation of the equipment occurs under the action of loads as such rather than due to hydrogen dissolved in the steel. This effect is observed in all the three investigated cases of equipment damage despite their different media (organic and inorganic substances), as well as different operating pressures and operating temperatures.
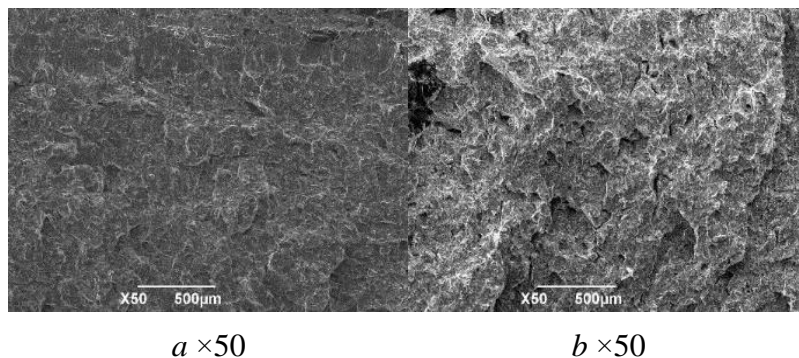

a ×50   *b* ×50

Fig. 4. Electron microscopic images of sample fractures after impact bending:
sample No 1D (*a*); sample No 1N (*b*)

Table 5

Carbon concentration on fractures of samples, %

Sample number	Sample No 1D	Sample No 1N
Field No 1	1.66	0.66
Field No 2	1.58	0.64
Field No 3	1.59	0.67
Field No 4	1.65	0.66
Field No 5	1.60	0.63
Average value	1.62	0.65

It should be noted that decarburization of structural steels under thermo-mechanical load is a well-studied process [33–35]. With a single-step annealing or normalization, it occurs at a depth of about 40 мм [23, 26]. The mechanism of decarburization under load is associated with the thermal decomposition of pearlite, carbides, and martensite, followed by the diffusion of carbon atoms onto

grain boundaries and onto the free surface of the metal. This is facilitated by a relatively high diffusion coefficient of carbon atoms in iron and external mechanical loads [20, 36].

The main chemical reactions of decarburization in this case are as follows [36]:

$$2C + O_2 \rightarrow 2CO \tag{3}$$
$$C + H_2O \rightarrow CO + H_2 \tag{4}$$
$$C + FeO \rightarrow Fe + CO. \tag{5}$$

To protect steels from such carbon loss, gas-tight and heat-resistant coatings of workpieces are used before annealing or quenching, for example, aluminum-silicon compounds [13]. Heat treatment in a protective reducing environment is also used [20].

Thus, the process of decarburization of steel grains under load proceeds precisely from inside the grains to the boundaries, followed by the formation of carbon monoxide and molecular hydrogen during the reactions of carbon with oxygen, iron oxides, and water molecules. It should be noted that in the cases studied we observed exactly the same carbon diffusion. Thus, it is not hydrogen that leads to decarburization, but the decomposition of carbon compounds in steels under thermo-mechanical load and carbon diffusion lead to additional accumulation of hydrogen and further decarburization "on average" if oxygen enters these boundaries or if they are contaminated with iron oxides.

With such a basic decarburization mechanism, there remains only one contradiction with the numerous observations of the consequences of a high-temperature hydrogen attack. Unclear is the mechanism of formation of methane and other hydrocarbons in defects in the microstructure of steels, which are often observed (see, for example, [14]).

It is known from the general course of organic chemistry that even in the presence of catalysts, the direct reaction of hydrogen with carbon does not occur. Well-studied coal gasification reactions can only be written in the most generalized form as a direct reaction of hydrogen with carbon [37]. The formation of methane occurs as a result of a chain of reactions occurring only in the presence of additional reagents, for example, carbon monoxide or an organic solvent [37]. Moreover, at high temperatures (above 1000 °C), methane is highly likely to decompose into carbon and hydrogen, and metal catalysts can reduce the decomposition temperature (pyrolysis of methane) to 450–500 °C.

Using well-researched methods of industrial production of methane, one can suggest that the following main reactions take place at the grain boundaries during the decarburization of steels: the direct reaction of carbon monoxide with hydrogen, known as a side reaction in the Fischer–Tropsch process [38, 39] (both gases are formed during decarburization),

$$CO + 3H_2 \rightarrow CH_4 + H_2O, \tag{6}$$

the formation of carbon dioxide from carbon monoxide and water molecules to form hydrogen,

$$CO + H_2O \rightarrow CO_2 + H_2, \tag{7}$$

and the subsequent Sabatier reaction [40, 41], which results in the synthesis of methane,

$$CO_2 + 4H_2 \rightarrow CH_4 + 2 H_2O. \tag{8}$$
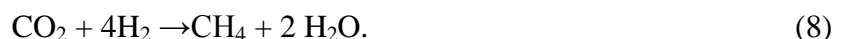
An important feature of these reactions, which lead to decarburization, is that hydrogen involved in them accumulates and is consumed during chemical reactions at the boundaries of metal grains, and it is not adsorbed from the environment. This allows us to explain why, with a huge difference in the carbon concentrations observed in steels and the concentrations of absorbed hydro-

gen, a significant portion of carbon is converted into methane and other more complex organic compounds.

A careful study of the primary sources shows that, since the first work known to us [4], hydrogen-induced decarburization has been studied on isolated samples artificially saturated with hydrogen under high pressure or by cathodic polarization. Under these conditions, the Nelson diagram and other patterns related to the phenomenon of decarburization during high-temperature hydrogen attack and with the development of hydrogen brittleness were obtained. The presence of specific surface effects [42] during artificial saturation of metals with hydrogen, including the hydrogen skin effect, does not allow these data to be used for long-term operation of industrial equipment without additional research and testing. Ignoring this circumstance may cause the unpredictable development of hydrogen brittleness and hydrogen-induced destruction of reactor walls, pipelines, and other industrial equipment.

4. Conclusion

Steel samples cut out from the walls of equipment damaged as a result of hydrogen embrittlement during operation in various hydrogen-containing media and at different operating pressures and temperatures have been studied with the application of various techniques. Direct measurement of hydrogen concentration has shown that, compared with the metal in the state of delivery, hydrogen concentration increases many times during operation of the equipment, and this, according to generally accepted concepts, leads to decarburization of the internal microstructure of steel grains. At the same time, in all the investigated cases of operational damage to the steel walls of the equipment, there is no complete removal of carbon from the steels as a result of hydrogen embrittlement. Besides, there is no decrease in the carbon concentration (average throughout the wall thickness), it is at the upper permissible level for all the studied steel grades. It has been found that carbon diffuses from the body of pearlite grains and accumulates along their boundaries. This effect has been observed in all the samples, despite a significant difference in the composition, temperatures, and pressures of the working medium. The maximum recorded carbon concentration has been observed at the grain boundaries, and it amounts to 11.5%. At that, the value of carbon concentration along the grain boundaries corresponds to the level of decarburization of the pearlite grains of the studied samples.

The analysis of the results allows us to make a reasonable assumption that the decomposition of pearlite and the diffusion of carbon under the influence of external thermo-mechanical loads, followed by its interaction with oxygen, iron oxides, and water at the grain boundaries, are an internal source of hydrogen ingress into the steel and methane formation with its participation. Thus, the methane disease of steels in the studied cases is a consequence of carbon diffusion to the grain boundaries rather than of hydrogen adsorption from the environment.

The discovered mechanism of steel degradation allows us to explain many contradictions, for example, a large difference in the concentrations of dissolved hydrogen and carbon in steels and the possibility of the development of hydrogen brittleness at low pressures and concentrations of hydrogen in the working environment, at relatively low operating temperatures of several hundred degrees Celsius. The long service life under load, apparently, is the main reason for the differences found in the microstructure of the steels as compared to the well-known published data obtained in studies of hydrogen-saturated samples under laboratory conditions.

References

1.   Archakov, Yu.I. *Vodorodnaya korroziya stali* [Hydrogen Corrosion of Steel]. Metallurgiya Publ., Moscow, 1985, 192 p. (In Russian).
2.   Kolachev, V.A. *Vodorodnaya khrupkost metallov* [Hydrogen Brittleness of Metals]. Metallurgiya Publ., Moscow, 1985, 216 p. (In Russian).

3. RD 10–577–03. Model guidelines for inspection of metal and prolongation of the service life of main components of boilers, turbines, and piping systems of thermal power stations. (In Russian).

4. Snoek, J.L. On the decarburization of steel and related questions. *Physica*, 1941, 8 (7), 734–744. DOI: 10.1016/S0031-8914(41)90536-0.

5. Sergeev, N.N., Chukanov, A.N., Baranov, V.P., and Yakovenko, A.A. Development of damage and decarburization of high-strength low-alloy steels under hydrogen embrittlement. *Metal Science and Heat Treatment*, 2015, 57, 63–68. DOI: 10.1007/s11041-015-9836-z.

6. Sergeev, N.N., Sergeev, A.N., Kutepov, S.N., Chukanov, A.N., Gvozdev, A.E., Tikhonova, I.V., and Shatulsky, A.A. Features of the process of local decarbonization of reinforcing steels during hydrogen cracking tests. *Vestnik RGATU im. P.A. Solovyeva*, 2019, 2, 79–86. (In Russian).

7. Gorchakov, L.N., Dobrotvorsky, A.M., Romanova, L.M., and Valkovskaya, S.A. Influence of hydrogen pressure on the mechanism of hydrogen corrosion of carbon steel. *Khimicheskaya Tekhnika*, 2016, 1, 16–19. (In Russian).

8. Kuzyukov, A.N., Borisenko, V.A., and Nikhaenko, Yu.Ya. Hydrogen corrosion of steels under anomalous conditions. *Tyazheloe Mashinostroenie*, 2005, 11, 36–37. (In Russian).

9. Bubnov, S.A., Ovchinnikov, I.I., and Bubnov, A.A. Investigation of destruction and decarburization kinetics of a thick-walled tubes under hydrogen corrosion. *Vestn. Sam. Gos. Tekhn. Un-ta, Ser. Fiz.-Mat. Nauki*, 2012, 16 (2), 178–182. (In Russian).

10. Jing, Y.A., Yuan, Y.M., Yan, X.L., Zhang, L., and Sha, M.H. Decarburization mechanism during hydrogen reduction descaling of hot-rolled strip steel. *International Journal of Hydrogen Energy*, 2017, 42 (15), 10611–10621. DOI: 10.1016/j.ijhydene.2017.01.230.

11. Xu, K. Hydrogen embrittlement of carbon steels and their welds. In: *Gaseous Hydrogen Embrittlement of Materials in Energy Technologies*, Woodhead Publishing, 2012, vol. 2, pp. 526–561. DOI: 10.1533/9780857093899.3.526.

12. Dayal, R.K. and Parvathavarthini, N. Hydrogen embrittlement in power plant steels. *Sadhana*, 2003, 28, 431–451. DOI: 10.1007/BF02706442.

13. Cho, L., Bradley, P.E., Lauria, D.S., Connolly, M.J., Seo, E.J., Findley, K.O., Speer, J.G., Golem, L., Slifka, A.J. Effects of hydrogen pressure and prior austenite grain size on the hydrogen embrittlement characteristics of a press-hardened martensitic steel. *International Journal of Hydrogen Energy*, 2021, 46 (47), 24425–24439. DOI: 10.1016/j.ijhydene.2021.05.005.

14. Lunarska, E., Nikiforow, K., and Pyrza, J. Hydrogen induced blistering cracking of steel at exploitation in boilers. *Mezdunarodnyi Nauchnyi Zhurnal Alternativnaya Energetika i Ekologiya*, 2006, 7 (39), 45–47. (In Russian).

15. Suranov, G.I., Latyshev, A.A., Karmanova, O.M., and Vasiliev, V.V. Study of the process of cathode hydrogenation of the samples and composition of evolved gas. *Zavodskaya Laboratoriya. Diagnostika Materialiov,* 2015, 81 (2), 20–24. (In Russian).

16. Barrera, O. and Cocks, A.C.F. Computational modelling of hydrogen embrittlement in welded structures. *Philosophical Magazine*, 2013, 93 (20), 2680–2700. DOI: 10.1080/14786435.2013.785638.

17. Gutzeit, J. and Thygeson, J.R.Jr. Effect of moisture on decarburization and fissuring of steel by hydrogen at elevated temperatures and pressures. *Corrosion*, 1967, 23 (10), 318–325. DOI: 10.5006/0010-9312-23.10.318.

18. Chun, Y.S., Kim, J.S., Park, K.-T., Lee, Y.-K., and Lee, C.S. Role of ε martensite in tensile properties and hydrogen degradation of high-Mn steels. *Materials Science and Engineering: A*, 2012, 533, 87–95. DOI: 10.1016/j.msea.2011.11.039.

19. Okuno, K. and Takai, K. Determination of hydrogen diffusibility and embrittlement susceptibility of high-strength steel evaluated at different temperatures based on the local equilibrium theory. *Acta Materialia*, 2023, 246, 118725. DOI: 10.1016/j.actamat.2023.118725.

20. Gojić, M., Kosec, L., and Matković, P. Embrittlement damage of low alloy Mn–V steel. *Engineering Failure Analysis*, 2003, 10 (1), 93–102. DOI: 10.1016/S1350-6307(02)00038-9.

21. Pinson, M., Claeys, L., Springer, H., Bliznuk, V., Depover, T., and Verbeken, K. Investigation of the effect of carbon on the reversible hydrogen trapping behavior in lab-cast martensitic Fe–C steels. *Materials Characterization*, 2022, 184, 111671. DOI: 10.1016/j.matchar.2021.111671.

22. Depover, T. and Verbeken, K. The key role of dedicated experimental methodologies in revealing the interaction between hydrogen and the steel microstructure. In: V.A. Polyanskiy, A.K. Belyaev, eds. *Advances in Hydrogen Embrittlement Study*, Springer, Cham, 2021, vol. 143, pp. 59–85. DOI: 10.1007/978-3-030-66948-5_5.

23. Zhang, T., Long, H., Cheng, G., Guo, J., Lei, Z., and Xun, Z. Cause of bending fracture in high-strength fasteners and heredity of surface recarburization in high carbon steel. *Engineering Failure Analysis*, 2024, 160, 108230. DOI: 10.1016/j.engfailanal.2024.108230.

24. Lee, J.A. and Woods, S. Hydrogen embrittlement. NASA/TM-2016–218602, 2016, 62 p.

25. Hrdinová, H., Kreibich, V., Kudlačиek, J., and Hornнk, J. Hydrogen Embrittlement after surface treatments. In: B. Gapicski, M. Szostak, V. Ivanov, eds. *Advances in Manufacturing II*. Ser. Lecture Notes in Mechanical Engineering, Volume 4–Mechanical Engineering, Springer, Cham, 2019, pp. 266–275. DOI: 10.1007/978-3-030-16943-5_24.

26. Venezuela, J., Liu, Q., Zhang, M., Zhou, Q. and Atrens, A. A review of hydrogen embrittlement of martensitic advanced high-strength steels. *Corrosion Reviews*, 2016, 34 (3), 153–186. DOI: 10.1515/corrrev-2016-0006.

27. Nechaeva, A.V., Polyansky, V.A., Polyansky, A.M., Shalagaev, V.V., and Yakovlev, Yu.A. Root cause analysis of the brittle fracture of pipes of boiler heating surfaces after long-term operation. *Zavodskaya Laboratoriya. Diagnostika Materialov*, 2024, 90 (4), 53–65. DOI: 10.26896/1028-6861-2024-90-4-53-65. (In Russian).

28. Franzenyuk, I.V. and Franzenyuk, L.I. *Album of Microstructures of Cast Iron, Steel, Non-Ferrous Metals and their Alloys*. Akademkniga Publ., Moscow, 2004, 190 p. (In Russian).

29. Krishtal, M.M., Karavanova, A.A., Eremichev, A.A., and Yasnikov, I.S. On the reversibility of cementite decomposition upon the hydrogenation of carbon steel. *Doklady Physics*, 2009. 54 (4), 193–195. DOI: 10.1134/S1028335809040090.

30. Masanskii O.A., Tokmin A.M., Kasakov V.S. A study of the influence of operating conditions on the degradation of the structure of steel 14MoV63. *Zhurnal SFU. Tekhnika i Tekhnologii*, 2019, 12 (4), 427–432. DOI: 10.17516/1999-494X-0148. (In Russian).

31. Ababkov, N.V., Danilov, V.I., Smirnov, A.N., Popova, N.A., and Pimonov, M.V. Investigation of dislocation structure, internal stresses and redistribution of carbon atoms in the zone of localized deformation in structural steel 20. *Technical Physics*, 2024, 21 (1), 112–121. DOI: 10.1134/S1063784224700221.

32. Yuryev, A.A., Ivanov, Yu.V., Gromov, V.E., Panin, S.V., Kormyshev, V.E., and Rubannikova, Yu.A. The effect of long-term operation on the redistribution of carbon atoms in rails. *Fundamentalnye Problemy Sovremennogo Materialovedeniya,* 2020, 17 (4), 449–455. DOI: 10.25712/ASTU.1811-1416.2020.04.006. (In Russian).

33. Wang, H., Su, F., and Wen, Z. Study on decarburization mechanism and law of GCr15 bearing steel during heat treatment. In: *Advances in Materials Science and Engineering*, Wiley, 2022, vol. 2022, no. 1, pp. 1–11. DOI; 10.1155/2022/3723680.

34. Biront, V.S. and Blokhin, I.V. Some features of phase transformations in iron-carbon system. *Zhurnal SFU. Tekhnika i Tekhnologii*, 2009, 2 (3), 238–249. (In Russian).

35. Biront, V.S. and Krushenko, G.G. Effect of heat and thermo-cyclic treatment on structure and properties of martensitic-ageing steel. *Zhurnal SFU. Tekhnika i Tekhnologii*, 2008, 1 (3), 247–255. (In Russian).

36. Choi, S. and Van Der Zwaag, S. Prediction of decarburized ferrite depth of hypoeutectoid steel with simultaneous oxidation. *ISIJ International*, 2012, 52 (4), 549–558. DOI: 10.2355/isijinternational.52.549.

DREAM
http://dream-journal.org

Diagnostics, Resource and Mechanics of materials and structures
Issue 1, 2025

22

http://dream-journal.org

ISSN 2410-9908

37. Petrov, I.Ya., Ushakov, K.Yu., Bogomolov, A.R., and Tryasunov, B.G. Catalytic liquefaction of coals is a promising method for the production of motor fuels and valuable chemical compounds. Part 2. The structure of coals and the chemistry of their direct liquefaction processes. *Vestnik KuzGTU*, 2020, 5 (141), 33–46. DOI: 10.26730/1999-4125-2020-5-33-46. (In Russian).

38. Dry, M.E. and Hoogendoorn, J.C. Technology of the Fischer-Tropsch process. *Catalysis Reviews, Science and Engineering*, 1981, 23, 1–2, 265–278. DOI: 10.1080/03602458108068078.

39. Dry, M.E. The Fischer–Tropsch process: 1950–2000. *Catalysis Today*, 2002, 71 (3–4), 227–241. DOI: 10.1016/S0920-5861(01)00453-9.

40. Vogt, C., Monai, M., Kramer, G.J., and Weckhuysen, B.M. The renaissance of the Sabatier reaction and its applications on Earth and in space. *Nature Catalysis*, 2019, 2 (3), 188–197. DOI: 10.1038/s41929-019-0244-4.

41. Chen, S., Abdel-Mageed, A.M. Methanation reactions for chemical storage and purification of hydrogen: Overview and structure-reactivity correlations in supported metals. *International Journal of Hydrogen Energy*, 2023, 48 (64), 24915–24935. DOI: 10.1016/j.ijhydene.2022.12.196.

42. Polyanskiy, V.A., Belyaev, A.K., Alekseeva, E.L., Polyanskiy, A.M., Tretyakov, D.A., and Yakovlev, Yu.A. Phenomenon of skin effect in metals due to hydrogen absorption. *Continuum Mechanics and Thermodynamics*, 2019, 31, 1961–1975. DOI: 10.1007/s00161-019-00839-2.